Available online at www.sciencedirect.com
ScienceDirect
Trans. Nonferrous Met. Soc. China 35(2025) 3824−3835
Transactions of Nonferrous Metals Society of China
www.tnmsc.cn

Machine learning on glass-forming ability of metallic glasses guided by domain knowledge

Hong BO[1], Xu-dong CHEN[1], Li-bin LIU[2], Xiao-gang FANG[1], Jian-liang HU[3], Li-min WANG[1]

1. State Key Laboratory of Metastable Materials Science and Technology, Yanshan University, Qinhuangdao 066004, China;
2. School of Materials Science and Engineering, Central South University, Changsha 410083, China;
3. College of Mechanical Engineering, Yanshan University, Qinhuangdao 066004, China

Received 12 March 2024; accepted 2 September 2024

Abstract: To improve the accuracy of machine learning in predicting the glass-forming ability, the atomic size difference, mixing enthalpy and estimated viscosity at liquidus temperature were selected as features from the perspectives of structure, thermodynamics and kinetics. Various algorithms including random forest (RF), extreme gradient boosting (XGBoost), and multilayer perceptron (MLP), were employed to predict the maximum size of the metallic glasses. Results show that the XGBoost models using the original and augmented datasets both exhibit superior performance, with the latter achieving the highest determination coefficient of 0.9148 among all the models. For predicting the maximum sizes of unseen Zr−Cu−Ni−Al−(Y) alloys, the XGBoost model trained on the augmented dataset demonstrates the best agreement with the measured data, indicating excellent generalization ability. By model interpretation, it is found that the kinetic factor correlates more with glass-forming ability compared with the thermodynamic and structural factors.

Key words: machine learning; extreme gradient boosting (XGBoost); Zr−Cu−Ni−Al−Y alloys; glass-forming ability; data augmentation

1 Introduction

The formation of metallic glasses has been commonly attributed to the combined effects of structure, thermodynamics, and kinetics. However, the available design methods or criteria for predicting glass-forming ability rarely take into account all the influential factors as mentioned above, making it difficult to predict the glass-forming ability accurately.

In recent years, significant progress has been made in the accelerated design of materials driven by computation and big data, thanks to the advanced concept of materials genome engineering. Machine learning, as a crucial tool, has found widespread applications in the composition design and property prediction of metallic glasses, greatly reducing the research and development cycle of novel materials with high performance [1−5]. SUN et al [6] analyzed the glass-forming ability of binary alloys via machine learning using the support vector machine (SVM) algorithm, and new binary alloys with good predicted glass-forming ability were suggested. LIU et al [7] studied the glass formation utilizing a back propagation neural network (BPNN) model based on a dataset of binary and ternary alloys, and generalized it to the multicomponent alloys with a high predictive accuracy of 83%. XIONG et al [8] employed the random forest (RF)

Corresponding author: Hong BO, Tel: +86-335-8057047, E-mail: bohong@ysu.edu.cn
https://doi.org/10.1016/S1003-6326(25)66915-9

algorithm to predict the glass-forming ability, the critical diameter, shear modulus and bulk modulus. Mathematical expressions were obtained from symbolic regression and three linear least-square models. LU et al [9] predicted the soft magnetism property and thermal stability of Fe-based metallic glasses using the extreme gradient boosting (XGBoost) model, which well predicted the saturation flux density and onset crystallization temperature with accuracy of 93.0% and 94.3%, respectively. Recently, ZHANG et al [10] proposed a fused strategy, developing the RF, k-nearest neighbor (KNN), gradient boosted decision trees (GBDT) and XGBoost models with the feature vectors extracted by the trained convolutional neural network (CNN) model. The fused models exhibit higher prediction accuracy than the four models mentioned above. For machine learning, the appropriateness of the selected features directly influences the predictive accuracy. In most studies [11−13], researchers selected the physical or thermodynamic properties of the alloys as input features, including valence electron concentration, electronegativity, liquidus temperature, and mixing enthalpy, etc. Due to the large number of features, feature selection is essential to obtain excellent predictions. However, these features normally have no strong and direct relation to glass formation, making it challenging to further enhance the predictive accuracy.

In fact, domain knowledge could facilitate the selection of the features [14,15], which helps to reduce the number of the features and the complexity of the model, thus avoiding overfitting and improving the generalization ability. Our objective is to utilize domain knowledge to guide the selection of features and predict the glass-forming ability of metallic glasses accurately via machine learning. We only selected three features as input, namely, atomic size difference, mixing enthalpy, and estimated viscosity at liquidus temperature, representing the influence from structure, thermodynamics and kinetics on glass formation. Using such a minimal feature set in machine learning to cover the influential factors comprehensively has not been achieved previously. Various models will be trained in this work and then used to predict the maximum sizes of the Zr−Cu−Ni−Al−(Y) alloys that are beyond the dataset for verification of their performance.

2 Methodology

2.1 Dataset

The compositions and maximum diameters of 456 bulk metallic glasses produced via copper mold suction casting are collected from the literature [16], and listed in Table S1 in the Supplementary Material. This dataset is both diverse and representative by including the majority of the constituent elements of the metallic glass systems. The maximum size, denoted as D_{max}, ranges from 1 to 50 mm, excluding amorphous ribbons with a thickness less than 1 mm. The distribution of maximum casting diameters in the dataset is illustrated in Fig. 1.

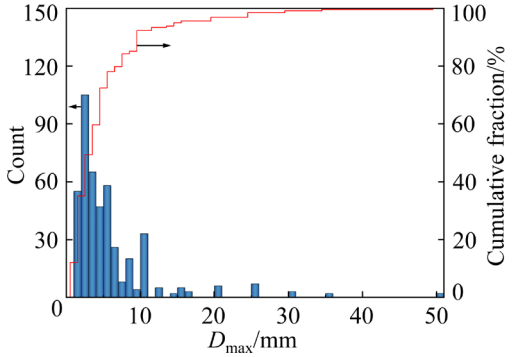

Fig. 1 Distribution of maximum diameter (D_{max}) in dataset

Based on domain knowledge, glass formation is primarily influenced by three mutually independent factors, namely structural, thermodynamic and kinetic factors [17−19]. We attempted to extract three features, each representing one influential factor, in order to enhance the accuracy of the machine learning predictions.

EGAMI and WASEDA [20] proposed that the ability to form amorphous alloys was related to large atomic size difference. TAKEUCHI and INOUE [21,22] calculated the mixing enthalpy and mismatch entropy for ternary amorphous alloys, finding that the values for most of these alloys fell within a trapezoid region in the plot of mixing enthalpy versus the mismatch entropy normalized by the Boltzmann constant. Here, the mismatch entropy is in proportional to the atomic size difference [23]. Many researchers [24,25] have used the atomic size difference (δ) and mixing enthalpy (H_{mix}) as features for machine learning, all of which

have achieved good results. Therefore, they were selected as structural and thermodynamic features in this work and can be calculated using Eqs. (1) and (2).

$$\delta=\sqrt{\sum_{i=1}^{n}c_i\left(1-r_i/\overline{r}\right)^2} \tag{1}$$

where $\overline{r}=\sum_{i=1}^{n}c_i r_i$, c_i and r_i are the atomic fraction and atomic radius of the ith element, respectively, and n is the number of alloying elements.

$$H_{\mathrm{mix}}=4\sum_{i=1,i<j}^{n}\Delta H_{ij}c_i c_j \tag{2}$$

where n is the number of binary sub-systems, and ΔH_{ij} is the molar mixing enthalpy for binary liquid alloys, which was adopted from literature [22].

Kinetically, high viscosity does not favor the nucleation and growth of the crystalline phase, thus leading to the formation of the amorphous state more easily. Previous studies [26−28] have revealed that the viscosity (η) at liquidus temperature closely relates to the glass-forming ability, with most bulk metallic glasses possessing a viscosity larger than 0.01 Pa·s. Therefore, this parameter is selected as the kinetic feature for machine learning. For a multi-component liquid, viscosity modeling was reported in our previous work [28,29], described by Eqs. (3) and (4).

$$\eta=\exp\left(\frac{Q'}{RT}\right) \tag{3}$$

where $Q'=RT\ln\eta_0+Q$, η_0 is the pre-exponential factor, Q is the activation energy, R is the molar gas constant, and T is the thermodynamic temperature. Q' can be expressed as a function of composition in the form of a Redlich−Kister polynomial as follows:

$$Q'=\sum_i x_i Q_i+\sum_i\sum_{j>i}x_i x_j\left(\sum_{r=0,1,2,\cdots}{}^{(r)}Q_{i,j}\left(x_i-x_j\right)^r\right)+\sum_i\sum_{j>i}\sum_{k>j}x_i x_j x_k\left(\sum_{s=i,j,k,\cdots}v_{i,j,k}^{s}\,{}^{(s')}Q_{i,j,k}\right) \tag{4}$$

where x_i is the mole fraction of the pure component i; Q_i adopts the value of Q' when describing the viscosity of the pure component with Eq. (3); ${}^{(r)}Q_{i,j}$ and ${}^{(s')}Q_{i,j,k}$ are binary and ternary interaction parameters expressed as $A+BT$, where A and B need to be optimized. $v_{i,j,k}^{s}$ can be written as $v_{i,j,k}^{s}=x_s+(1-x_i-x_j-x_k)/3$, and s' equals 0, 1 and 2 when s equals i, j and k, respectively.

It should be noted that the second and third terms in Eq. (4), concerning the effect of the interaction between two or three components, should be determined by fitting experimental data on the viscosity of the binary and ternary alloys. Since the experimental data are limited, obtaining the interaction parameters is impossible. Therefore, we decided to use Eq. (3) and the first term of Eq. (4) to calculate the kinetic feature, omitting the interaction terms, which have less influence on the actual viscosity than the first term. They can roughly estimate the viscosity of the alloy at liquidus temperature, denoted as η_l.

2.2 Algorithm selection

Machine learning, as the core of artificial intelligence, has given rise to many learning algorithms after years of development, such as decision tree, Bayesian algorithms, support vector machines, random forests, artificial neural networks, and deep learning. In this work, the non-linear regression models including RF, XGBoost, and multilayer perceptron (MLP) were developed to predict the maximum diameter of metallic glasses.

The random forest model is commonly used for learning nonlinear relationships, often demonstrating excellent performance. It is a clustering algorithm based on decision trees, where each decision tree samples and learns independently. Subsequently, the trees vote to arrive at the final result. This approach effectively addresses the overfitting or underfitting problem associated with a single weak learner and has been widely applied in various fields. WARD et al [30] developed a general-purpose machine-learning framework with 145 features capable of capturing diverse physical or chemical properties. Using the random forest algorithm, they predicted the glass-forming ability of unassessed alloy systems, achieving an accuracy of 80.2%. Subsequently, they incorporated additional features to predict the glass-forming ability, critical casting diameter, and supercooled liquid range of amorphous alloys, yielding favorable results [31].

The XGBoost algorithm is a relatively new algorithm proposed by CHEN and GUESTRIN [32], who significantly improved the speed and efficiency of the decision tree algorithm. To date, it has been widely used in machine learning, generating impressive results. LI et al [33] collected 618 pieces of data and built different machine learning models to predict the magnetic properties of iron-based amorphous materials, using supercooled liquid region, theoretical melting point, theoretical density, mean atom radius, etc., as features. The results showed that the XGBoost model exhibited excellent predictive performance. In another study, XIONG et al [16] established several regression models to predict the maximum diameters of metallic glasses, and suggested that the performance of the XGBoost model was superior to other models.

Multilayer perceptron consists of three parts, namely input layer, hidden layer and output layer. The input layer receives the feature variables with different weights, which are then passed to the hidden layer for nonlinear weighting of the data. The final result is output from the output layer. ZHANG et al [34] collected 1888 pieces of data and built a convolutional neural network model for training, successfully predicting the glass formation ability of the alloys. The model exhibited satisfactory performance across all the different datasets used for testing. This demonstrates the great potential of neural network models in predicting the glass-forming ability.

2.3 Model training and evaluation

In this work, all the data were normalized and divided into a training set and a testing set. 90% of the total data were used for training model and tuning its parameters, while the remaining 10% of the data were reserved for testing. The data in the testing set are solely used to evaluate the accuracy and generalization of the model.

The values of the three input features, i.e., η_l, H_{mix} and δ, differ among each other by many orders of magnitude. In order to eliminate the effect of large difference, they were mapped to the range of 0−1 via normalization, typically using the formula as follows:

$$X=\frac{x-x_{\min}}{x_{\max}-x_{\min}} \tag{5}$$

where X is the normalized feature value, x is the actual feature value, and x_{max} and x_{min} are the maximum and minimum values of the input feature, respectively.

This normalization ensures that all features contribute equally to the machine learning model.

The coefficient of determination (R^2), Pearson correlation coefficient (ρ) and root mean square error (RMSE) are used as metrics to evaluate the predictive performance of the model. They could be calculated by Eqs. (6)−(8).

$$R^2=1-\frac{\sum_{i=1}^{n}\left(y_i-\hat{y}_i\right)^2}{\sum_{i=1}^{n}\left(y_i-\overline{y}\right)^2} \tag{6}$$

$$\rho=\frac{\sum_{i=1}^{n}\left(y_i-\overline{y}\right)\left(\hat{y}_i-\overline{\hat{y}}\right)}{\sqrt{\sum_{i=1}^{n}\left(y_i-\overline{y}\right)^2\sum_{i=1}^{n}\left(\hat{y}_i-\overline{\hat{y}}\right)^2}} \tag{7}$$

$$\mathrm{RMSE}=\sqrt{\frac{1}{n}\sum_{i=1}^{n}\left(y_i-\hat{y}_i\right)^2} \tag{8}$$

where y_i and $\hat{y}_i$ are the true and predicted values, respectively; $\overline{y}$ and $\overline{\hat{y}}$ are the mean values of y_i and $\hat{y}_i$, respectively.

3 Result and discussion

3.1 Regression results

The predictive results from the RF model are presented in Fig. 2. The optimized RF model achieves a coefficient of determination of 0.9012, a Pearson correlation coefficient of 0.9634, and a root mean square error of 1.9860 in the training set, while they turn out to be 0.8914, 0.9464 and 1.8198, respectively, for the testing set. The figure reveals that the model's predictions are more accurate when the maximum casting sizes are not more than 10 mm, since data in this range appear denser than those outside the range.

The predicted results from the XGBoost model are shown in Fig. 3. The coefficient of determination and the Pearson correlation coefficient of the training set reach 0.9662 and 0.9867, respectively, with a RMSE of 1.2313. For the testing set, the first two values drop to 0.9115 and 0.9607, and the RMSE increases to 1.6012. In comparison to the RF model, the XGBoost model

demonstrates consistent performance across the entire range of the maximum size for both the training and testing sets, suggesting minimal impact from data imbalance.

Figure 4 shows the training and testing results of the multilayer perceptron model. After tuning

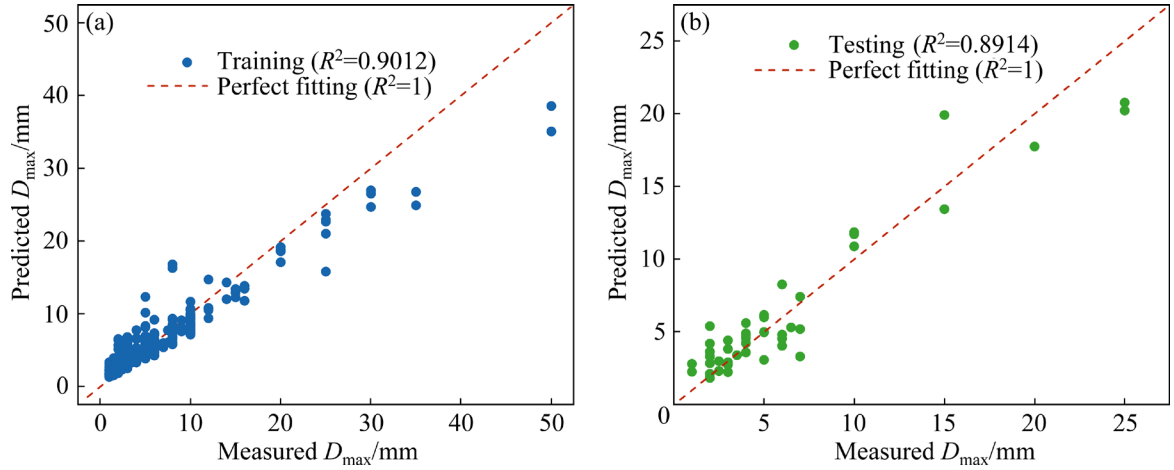

Fig. 2 Predicted D_{max} with RF model on training (a) and testing (b) data

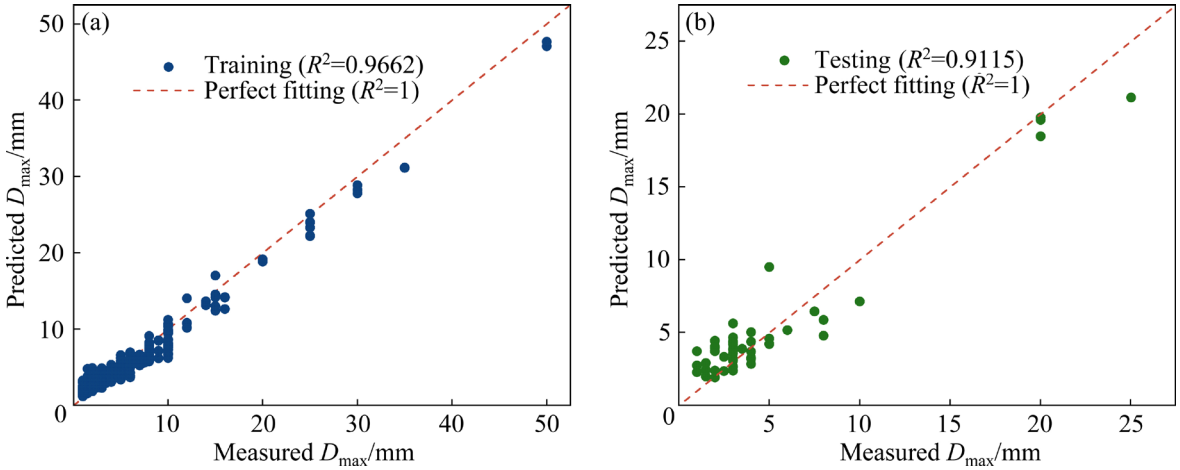

Fig. 3 Predicted D_{max} with XGBoost model on training (a) and testing (b) data

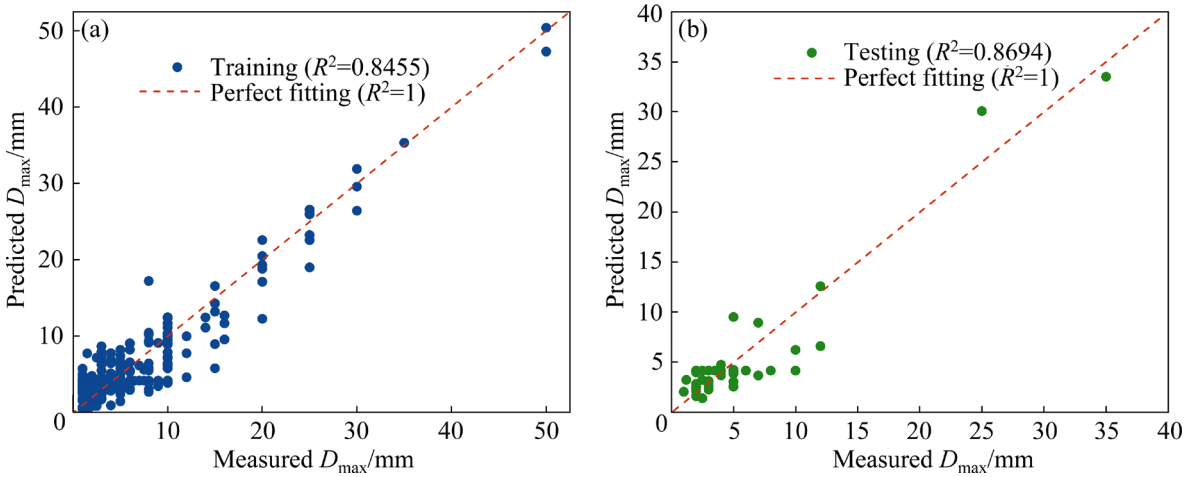

Fig. 4 Predicted D_{max} with MLP model on training (a) and testing (b) data

parameters, the coefficient of determination and the Pearson correlation coefficient of the training set achieve 0.8455 and 0.9195, respectively. The root mean square error is 2.4545. For the testing set, these metrics are 0.8694, 0.9352, and 2.1572, respectively. The predictive performance is even not good as that of the RF model.

In the light of the imbalance in dataset as previously mentioned, we conducted data augmentation in order to further improve the prediction precision of the model. Synthetic minority oversampling technique (SMOTE) is extensively used to solve the classification problem for an imbalanced dataset [35,36]. SMOTE for regression (SMOTER) [37] and synthetic minority oversampling with Gaussian noise (SMOGN) [38] have been developed to solve the regression problem recently. They were implemented in the work of XIONG and ZHANG [11], and helped to improve the performance of regression model to certain extent. In this work, the original data were augmented with the SMOGN technique, which produced an additional 155 pieces of data. The distribution of the augmented data produced by SMOGN was displayed in Fig. 5 along with the original data. After augmentation, all the data were normalized and divided into training set and testing set, with a ratio of 9∶1. Considering the exceptional performance of the XGBoost model for the original dataset, it was also employed for the augmented one, getting a score of 0.631 in 10-fold cross-validation. Figure 6 presents the predicted D_{max} by XGBoost model after data augmentation. Compared with its previous performance shown in Fig. 3, one can notice that a better fit is obtained for the training dataset. A higher determination coefficient, a higher Pearson correlation coefficient and a lower root mean square error are achieved, with values of 0.9983, 0.9995 and 1.0101, respectively. For the testing dataset, the determination coefficient is 0.9148, which is slightly higher than that before augmentation. However, a similar Pearson correlation coefficient and a high root mean square are obtained, i.e. 0.9596 and 2.8024, respectively. This is mainly caused by the large discrepancy of very few data in the testing set especially the one with a measured D_{max} of 1mm and a predicted one of large than 10 mm, as shown in Fig. 6(b).

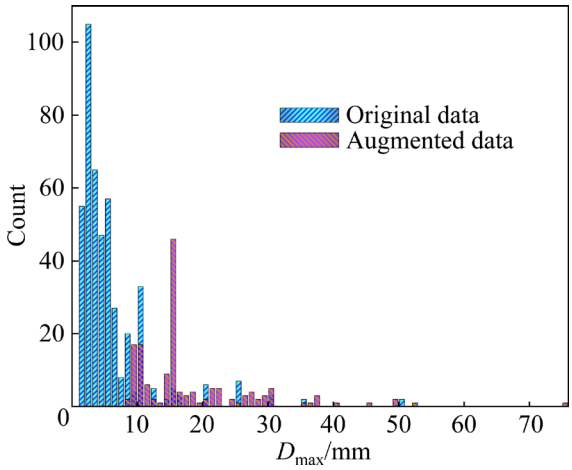

Fig. 5 Distribution of SMOGN data along with original data

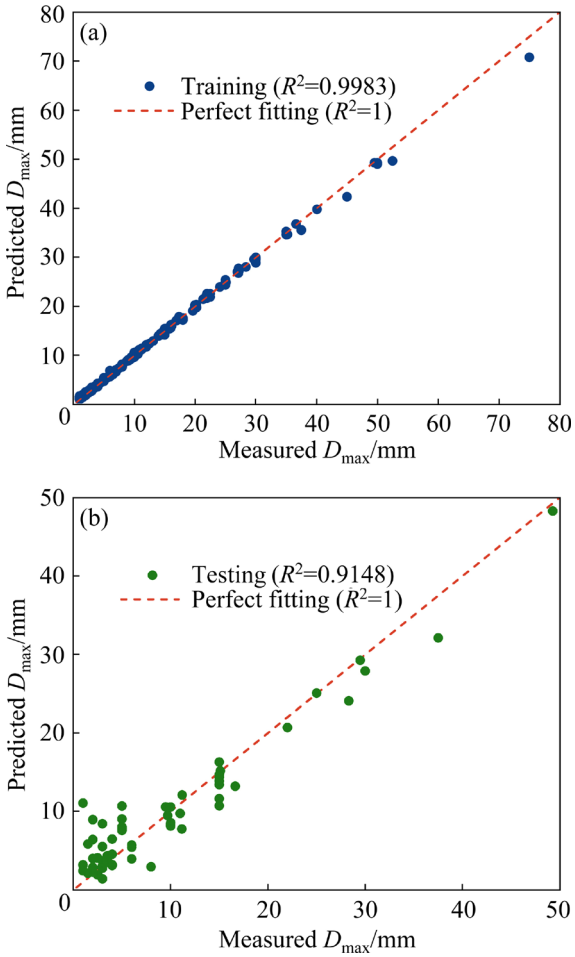

Fig. 6 Predicted D_{max} with XGBoost model on training (a) and testing (b) data after data augmentation

Table 1 lists the calculated R^2, ρ and RMSE using three different algorithms. It is evident that the XGBoost model using SMOGN data shows the highest R^2, demonstrating the best performance in

predicting the glass-forming ability of metallic glasses, followed by the XGBoost model using the original data, the RF model and the MLP model.

Table 1 Determination coefficient (R^2), Pearson correlation coefficient (ρ) and root mean square error (RMSE) of three algorithms

Algorithm	Dataset	R^2	ρ	RMSE
RF	Training set	0.9012	0.9634	1.9860
	Testing set	0.8914	0.9464	1.8198
XGBoost	Training set	0.9662	0.9867	1.2313
	Testing set	0.9115	0.9607	1.6012
MLP	Training set	0.8455	0.9195	2.4545
	Testing set	0.8694	0.9352	2.1572
XGBoost (SMOGN data)	Training set	0.9983	0.9995	1.0101
	Testing set	0.9148	0.9596	2.8024

3.2 Generalization capability of models

Using the models that have been trained, the maximum diameters of a series of alloys were predicted and compared with experimental results.

One Zr−Cu−Ni−Al alloy and six Zr−Cu−Ni−Al−Y alloys were arc-melted, using raw materials with a purity of 99.99 wt.% for all elements. The arc melting process was conducted at least four times in an argon atmosphere to achieve a homogeneous composition. Each alloy was then sectioned, with one piece used for melt quenching to produce amorphous ribbons at a wheel rate of 40 m/s. The amorphous state was confirmed through XRD, and DSC was employed to determine characteristic temperatures, such as phase transition temperature (T_g), crystallization temperature (T_x) and liquidus temperature (T_l). Using the measured liquidus temperature, η_l was calculated. Along with the other two calculated features, the maximum diameter could be predicted. Other pieces of the alloy were suction-cast into the copper mold to produce rods with diameters near the predicted values. Figure 7 displays the XRD patterns of the rods prepared by suction casting. As seen in Fig. 7(a), both $Zr_{42}Cu_{41}Ni_5Al_7Y_5$ and $Zr_{44.7}Cu_{28}Ni_9Al_{12.3}Y_6$ alloys possess a maximum diameter of 4 mm, as the crystalline peaks emerge for samples with a diameter of 5 mm. The maximum diameters of $Zr_{52}Cu_{28}Ni_8Al_{10}Y_2$ and $Zr_{50}Cu_{27}Ni_8Al_{10}Y_5$ alloys achieve 5 mm, showing negligible crystalline peaks. The XRD patterns of $Zr_{48.7}Cu_{28}Ni_9Al_{12.3}Y_2$ and $Zr_{46.7}Cu_{28}Ni_9Al_{12.3}Y_4$ alloys presented in Fig. 7(b) both show an amorphous state in the rods with a diameter of 12 mm. The former still remains amorphous basically when the diameter increases to 15 mm, while crystalline phases precipitate in the latter when it reaches 14 mm. Thus, the maximum diameter for the former is 15 mm, and for the latter, it is about 12 mm. Regarding the $Zr_{50.7}Cu_{28}Ni_9Al_{12.3}$ alloy, the reported critical diameter is 14 mm [39]. However, small crystalline peaks emerged on top of the characteristic diffuse peak of the amorphous phase in the sample with a diameter of 12 mm prepared in this work. The difference in the maximum diameter should be attributed to the difference in the cooling rate during the experiments, resulting from differences in the suction casting equipment or the experimental parameters. Regardless, the maximum diameter of this alloy was considered to be around 12 mm for the present study.

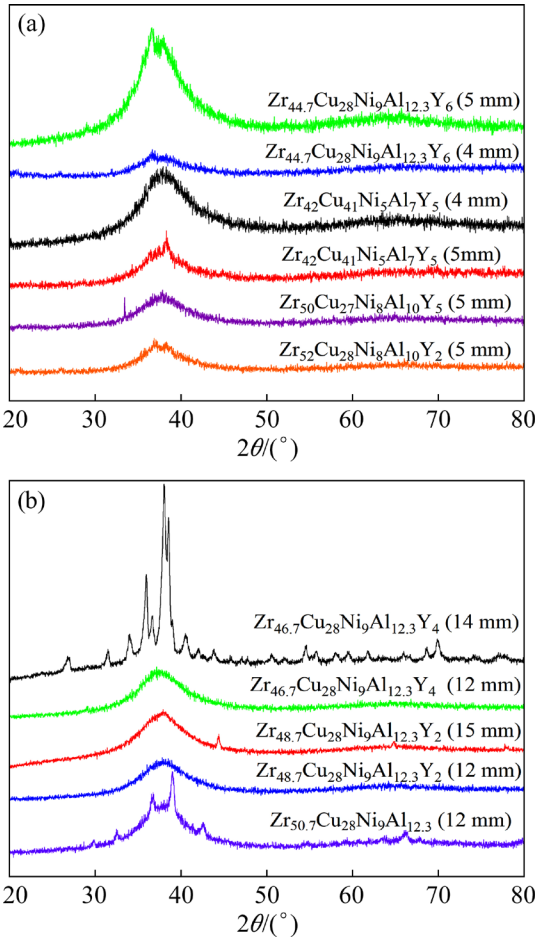

Fig. 7 XRD patterns of Zr−Cu−Ni−Al−(Y) alloy rods with different casting diameters

Table 2 Measured and predicted D_{max} of Zr−Cu−Ni−Al−(Y) bulk metallic glasses

Alloy composition	Measured D_{max}/mm	Predicted D_{max}/mm			
		RF	XGB	MLP	XGB (SMOGN data)
$Zr_{42}Cu_{41}Ni_5Al_7Y_5$	4	13	9	11	6
$Zr_{52}Cu_{28}Ni_8Al_{10}Y_2$	5	5	6	6	5
$Zr_{50}Cu_{27}Ni_8Al_{10}Y_5$	5	6	5	3	4
$Zr_{50.7}Cu_{28}Ni_9Al_{12.3}$	~12	8	11	13	10
$Zr_{48.7}Cu_{28}Ni_9Al_{12.3}Y_2$	15	12	17	17	14
$Zr_{46.7}Cu_{28}Ni_9Al_{12.3}Y_4$	12	8	8	9	13
$Zr_{44.7}Cu_{28}Ni_9Al_{12.3}Y_6$	4	6	6	5	5

Table 2 presents the measured and predicted D_{max} of the Zr−Cu−Ni−Al−(Y) bulk metallic glasses. A comparison reveals that a smaller difference exists between predicted and experimental values for the XGBoost model compared to the other two models before data augmentation, indicating its superior predictive ability. After augmentation, the XGBoost model shows even better prediction performance. This aligns with the earlier observation that it achieves high scores in both the training and testing sets. The superior performance may be attributed to the following advantages of the XGBoost model. It performs second-order Taylor expansion on the loss function, which allows the model to approach the real loss function more precisely. Besides, the adoption of the regularization could avoid overfitting and improve the generalization ability of the model. For the RF and MLP models, a large difference exists between the predicted and measured D_{max} value of $Zr_{42}Cu_{41}Ni_5Al_7Y_5$ alloy, 9 and 7 mm, respectively. These discrepancies may be attributed to the imbalance in the distribution of the data, which makes the model pay more attention to the samples in the dense region rather than those in the rare region during training, thus influencing the accuracy of the prediction. As can be seen from the prediction performance on training and testing data in Fig. 2 and Fig. 4, both the RF and MLP models tend to overestimate the maximum sizes of bulk metallic glasses when the measured data are smaller than 5 mm. Thus, it is understandable that they overestimate the D_{max} value of the $Zr_{42}Cu_{41}Ni_5Al_7Y_5$ alloy.

3.3 Model interpretation

The SHapley Additive exPlanation (SHAP), an approach based on the game theory, was employed to interpret the machine learning models used in this study. The SHAP value is utilized to represent the influence of each feature on a predicted result. The mean absolute value for a feature, considering the entire dataset, can be deemed as its impact on the target property.

Figure 8 displays the mean absolute SHAP values of three features with the RF, MLP and two XGBoost models. One can notice that the estimated viscosity at the liquid temperature (η_l) has the highest impact on predicting D_{max}, followed by the enthalpy of mixing (H_{mix}), and then the atomic size difference (δ). This indicates that the kinetic factor has the most influence on glass formation, followed by the thermodynamic and structural factor. The mean SHAP values for all three features are larger than 1 mm.

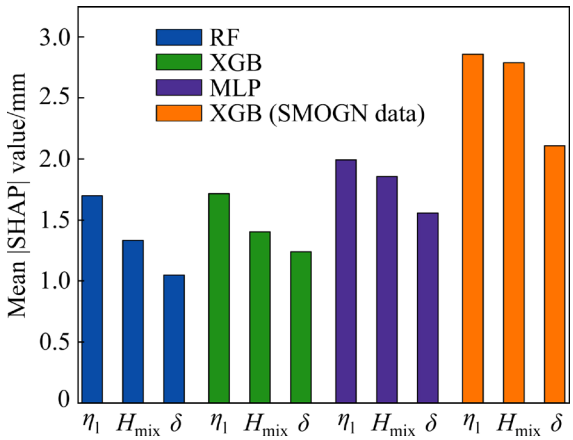

Fig. 8 Mean absolute SHAP values of three features with four models

Figure 9 presents the SHAP values for each datum in the dataset using the XGBoost model, providing insights into the impact of each feature.

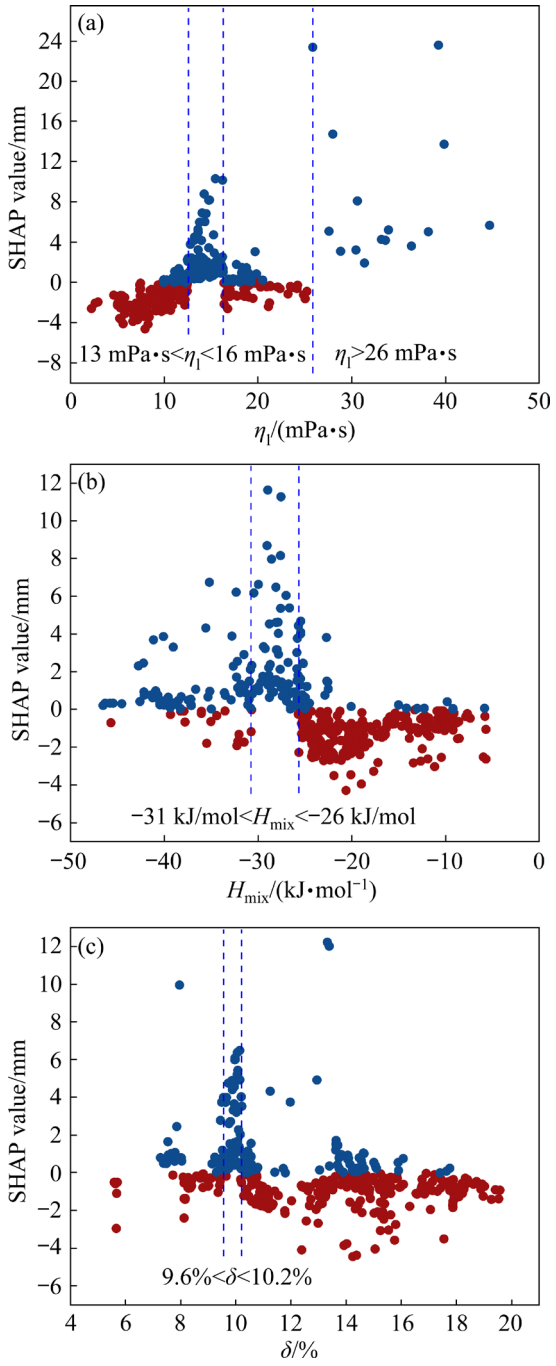

Fig. 9 SHAP values of each datum of estimated viscosity at liquidus temperature η_l (a), enthalpy of mixing H_{mix} (b), and atomic size difference δ (c) with XGBoost model

The SHAP values of η_l vary differently with the increase in the feature value compared to those of H_{mix} and δ. There are two ranges of positive SHAP values corresponding to η_l of 13−16 mPa·s and larger than 26 mPa·s. In Fig. 9 (b), the SHAP values are predominantly positive when H_{mix} falls from −31 to −26 kJ/mol, agreeing well with the range reported by XIONG and ZHANG [11]. The range for δ to obtain a positive SHAP value is extremely small, i.e., 9.6%−10.2%. The SHAP values for each datum using the XGBoost model after data augmentation are demonstrated in Fig. 10. It can be noted that distribution of the data is basically the same as that before augmentation, and so are the ranges for η_l, H_{mix} and δ with positive SHAP values.

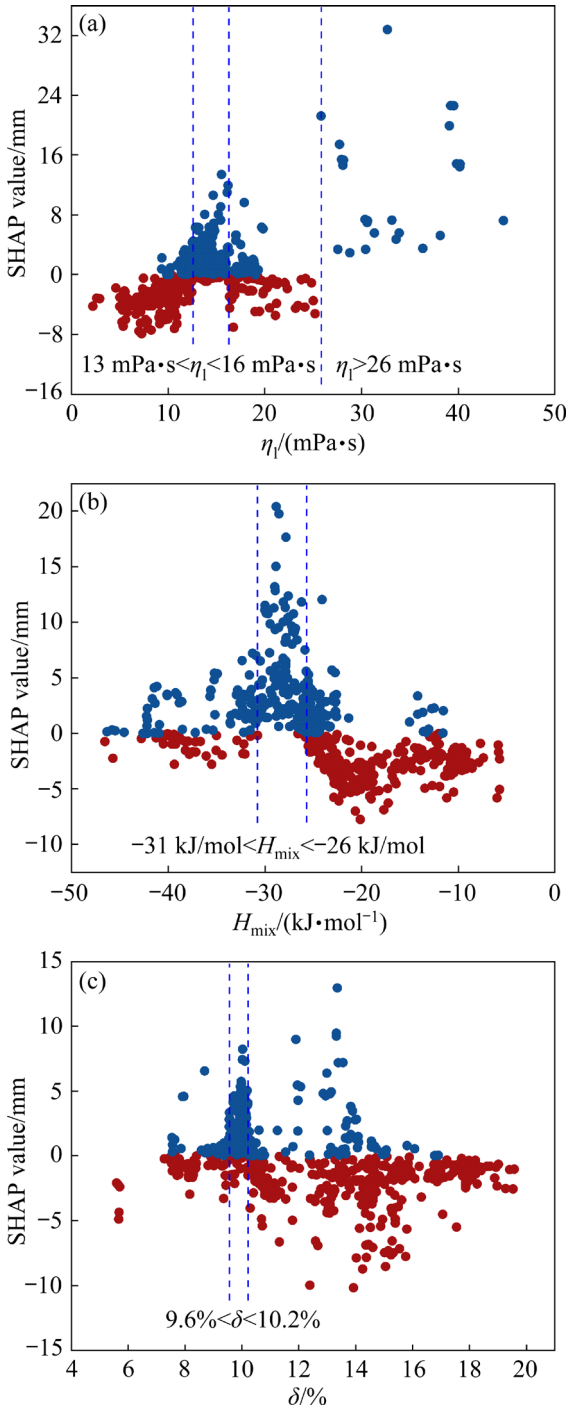

Fig. 10 SHAP values of each datum of estimated viscosity at liquidus temperature η_l (a), enthalpy of mixing H_{mix} (b), and atomic size difference δ (c) with XGBoost model after data augmentation

4 Conclusions

(1) Three features representing influences from structure, thermodynamics, and kinetics are selected, namely, atomic size difference, mixing enthalpy and estimated viscosity at liquidus temperature. Though with only three features, the RF, XGBoost, and MLP models can be trained to predict the maximum sizes of the metallic glasses with high accuracy.

(2) Using the original dataset, the XGBoost model possesses superior performance, achieving the highest determination coefficient of 0.9662 for the training set and 0.9115 for the testing set, followed by the RF model and then the MLP model.

(3) With the augmented dataset, the XGBoost model achieves the highest determination coefficient of 0.9983 for the training set and 0.9148 for the testing set. It also demonstrates the best performance when predicting the maximum sizes of the Zr−Cu−Ni−Al and Zr−Cu−Ni−Al−Y metallic glasses that are beyond the dataset, which indicates good generalization ability.

(4) Mean SHAP values of the three features for all the models are larger than 1 mm. Viscosity at liquidus temperature has the most significant impact on predicting D_{max}, followed by enthalpy of mixing, and then atomic size difference. This suggests that the kinetic factor has the greatest influence on glass formation, followed by the thermodynamic and structural factors.

(5) SHAP values of each datum reveal that it is favorable for glass formation when η_l falls in the range of 13−16 mPa·s or larger than 26 mPa·s, H_{mix} in the range of −31 to −26 kJ/mol, and δ between 9.6% and 10.2%.

CRediT authorship contribution statement

Hong BO: Conceptualization, Methodology, Data curation, Validation, Funding acquisition, Writing – Original draft; **Xu-dong CHEN:** Data curation, Investigation, Resources, Visualization; **Li-bin LIU:** Conceptualization, Writing − Review & editing; **Xiao-gang FANG:** Data curation, Investigation; **Jian-liang HU:** Conceptualization, Validation; **Li-min WANG:** Supervision, Funding acquisition, Writing – Review & editing.

Declaration of competing interest

The authors declare that they have no known competing financial interests or personal relationships that could have appeared to influence the work reported in this paper.

Data availability

The raw/processed data that supports the findings of this study is available from the corresponding author upon reasonable request.

Acknowledgments

This work was financially supported by the National Natural Science Foundation of China (No. 52171018), the National Key R&D Program of China (No. 2018YFA0703602), and Hebei Natural Science Foundation, China (No. E2021203059).

Supplementary Material

Supplementary Material in this paper can be found at: http://tnmsc.csu.edu.cn/download/18-p3824-2024-0399-Supplementary_Materials.pdf.

References

[1] REN F, WARD L, WILLIAMS T, LAWS K J, WOLVERTON C, HATTRICK-SIMPERS J, MEHTA A. Accelerated discovery of metallic glasses through iteration of machine learning and high-throughput experiments [J]. Science Advances, 2018, 4(4): eaaq1566.

[2] SARKER S, TANG-KONG R, SCHOEPPNER R, WARD L, HASAN N A, van CAMPEN D G, TAKEUCHI I, HATTRICK- SIMPERS J, ZAKUTAYEV A, PACKARD C E, MEHTA A. Discovering exceptionally hard and wear-resistant metallic glasses by combining machine-learning with high throughput experimentation [J]. Applied Physics Reviews, 2022, 9: 011403.

[3] LIU Guan-nan, SOHN S, KUBE S A, RAJ A, MERTZ A, NAWANO A, GILBERT A, SHATTUCK M D, O'HERN C S, SCHROERS J. Machine learning versus human learning in predicting glass-forming ability of metallic glasses [J]. Acta Materialia, 2023, 243: 118497.

[4] AMIGO N, PALOMINOS S, VALENCIA F J. Machine learning modeling for the prediction of plastic properties in metallic glasses [J]. Scientific Reports, 2023, 13: 348.

[5] LI Kang-yuan, LI Mao-zhi, WANG Wei-hua. Inverse design machine learning model for metallic glasses with good glass-forming ability and properties [J]. Journal of Applied Physics, 2024, 135: 025102.

[6] SUN Yi-tao, BAI Hai-yang, LI Mao-zhi, WANG Wei-hua. Machine learning approach for prediction and understanding of glass-forming ability [J]. The Journal of Physical Chemistry Letters, 2017, 8(14): 3434−3439.

[7] LIU Xiao-di, LI Xin, HE Quan-feng, LIANG Dan-dan, ZHOU Zi-qing, MA Jiang, YANG Yong, SHEN Jun. Machine learning-based glass formation prediction in multicomponent alloys [J]. Acta Materialia, 2020, 201:

182−190.

[8] XIONG Jie, SHI San-qiang, ZHANG Tong-yi. A machine-learning approach to predicting and understanding the properties of amorphous metallic alloys [J]. Materials & Design, 2020, 187: 108378.

[9] LU Zhi-chao, CHEN Xin, LIU Xiong-jun , LIN De-ye, WU Yuan, ZHANG Yi-bo, WANG Hui, JIANG Sui-he, LI Hong-xiang, WANG Xian-zhen, LU Zhao-ping. Interpretable machine-learning strategy for soft-magnetic property and thermal stability in Fe-based metallic glasses [J]. NPJ Computational Materials, 2020, 187(6): 1−9.

[10] ZHANG Ting, LONG Zhi-lin, PENG Li. Glass forming ability prediction of bulk metallic glasses based on fused strategy [J]. Transactions of Nonferrous Metals Society of China 2024, 34: 1558−1570.

[11] XIONG Jie, ZHANG Tong-yi. Data-driven glass-forming ability criterion for bulk amorphous metals with data augmentation [J]. Journal of Materials Science & Technology, 2022, 121: 99−104.

[12] PENG Li, LONG Zhi-lin, ZHAO Ming-sheng-zi. Determination of glass forming ability of bulk metallic glasses based on machine learning [J]. Computational Materials Science, 2021, 195: 110480.

[13] TANG Yi-chuan, HE Yi-fan, FAN Zhuo-qun, WANG Zhong-qi, TANG Cheng-ying. Highly effective design of high GFA alloys with different metal-based and various components by machine learning [J]. Science China Technological Sciences, 2024, 67: 1431−1442.

[14] LI Xin, SHAN Guang-cun, ZHAO Hong-bin, SHEK C H. Domain knowledge aided machine learning method for properties prediction of soft magnetic metallic glasses [J]. Transactions of Nonferrous Metals Society of China, 2023, 33: 209−219.

[15] LIU Yue, ZOU Xin-xin, MA Shu-chang, AVDEEV M, SHI Si-qi. Feature selection method reducing correlations among features by embedding domain knowledge [J]. Acta Materialia, 2022, 238: 118195.

[16] XIONG Jie, SHI San-qiang, ZHANG Tong-yi. Machine learning prediction of glass-forming ability in bulk metallic glasses [J]. Computational Materials Science, 2021, 192: 110362.

[17] HOSOKAWA S, BÉRAR J F, BOUDET N, PILGRIM W C, PUSZTAI L, HIROI S, MARUYAMA K, KOHARA S, KATO H, FISCHER H E, ZEIDLER A. Partial structure investigation of the traditional bulk metallic glass $Pd_{40}Ni_{40}P_{20}$ [J]. Physical Review B, 2019, 100: 054204.

[18] JOHNSON W L, NA J H, DEMETRIOU M D. Quantifying the origin of metallic glass formation [J]. Nature Communications, 2016, 7: 10313.

[19] WANG Li-min, TIAN Yong-jun, LIU Ri-ping, WANG Wei-hua. A “universal” criterion for metallic glass formation [J]. Applied Physics Letters, 2012, 100: 261913.

[20] EGAMI T, WASEDA Y. Atomic size effect on the formability of metallic glasses [J]. Journal of Non-Crystalline Solids, 1984, 64(1): 113−134.

[21] TAKEUCHI A, INOUE A. Calculations of mixing enthalpy and mismatch entropy for ternary amorphous alloys [J]. Materials Transactions JIM, 2000, 41(11): 1372−1378.

[22] TAKEUCHI A, INOUE A. Classification of bulk metallic glasses by atomic size difference, heat of mixing and period of constituent elements and its application to characterization of the main alloying element [J]. Materials Transactions, 2005, 46(12): 2817−2829.

[23] TAKEUCHI A, AMIYA K, WADA T, YUBUTA K, ZHANG W, MAKINO A. Entropies in alloy design for high-entropy and bulk glassy alloys [J]. Entropy, 2013, 15(9): 3810−3821.

[24] GUO Sheng, HU Qiang, CHUN NG, LIU C T. More than entropy in high-entropy alloys: Forming solid solutions or amorphous phase [J]. Intermetallics, 2013, 41: 96−103.

[25] DENG Bing-hui, ZHANG Ya-li. Critical feature space for predicting the glass forming ability of metallic alloys revealed by machine learning [J]. Chemical Physics, 2020, 538: 110898.

[26] MUKHERJEE S, SCHROERS J, JOHNSON W L, RHIM W K. Influence of kinetic and thermodynamic factors on the glass-forming ability of zirconium-based bulk amorphous alloys [J]. Physical Review Letters, 2005, 94: 245501.

[27] BAIRD J A, SANTIAGO-QUINONEZ D, RINALDI C, TAYLOR L S. Role of viscosity in influencing the glass-forming ability of organic molecules from the undercooled melt state [J]. Pharmaceutical Research, 2012, 29: 271−284.

[28] BO Hong, ZHANG Zhong-hua, HU Jian-liang, WANG Li-min. A new model on the viscosities of the Zr−Cu−Al liquid alloys [J]. Calphad, 2020, 71: 102208.

[29] BO Hong, ZHNAG Zhong-hua, WANG Li-min. Comparative study on the viscosity modeling of the Ag−Au−Cu liquid alloys [J]. Calphad, 2021, 73: 102270.

[30] WARD L, AGRAWAL A, CHOUDHARY A, WOLVERTON C. A general-purpose machine learning framework for predicting properties of inorganic materials [J]. NPJ Computational Materials, 2016, 2: 16028.

[31] WARD L, O’KEEFFE S C, STEVICK J, JELBERT G R, AYKOL M, WOLVERTON C. A machine learning approach for engineering bulk glass metallic glass alloys [J]. Acta Materialia, 2018, 159: 102−111.

[32] CHEN Tian-qi, GUESTRIN C. XGBoost: A scalable tree boosting system [C]//KRISHNAPURAM B, SHAH M, SMOLA A J, AGGARWAL C C, SHEN D, RASTOGI R. Proceedings of the 22nd ACM SIGKDD International Conference on Knowledge Discovery and Data Mining. San Francisco, CA: ACM, 2016: 785−794.

[33] LI Xin, SHAN Guang-cun, SHEK C H. Machine learning prediction of magnetic properties of Fe-based metallic glasses considering glass forming ability [J]. Journal of Materials Science & Technology, 2022, 103: 113−120.

[34] ZHANG Ting, LONG Zhi-lin, PENG Li, LI Zhuang. Prediction of glass forming ability of bulk metallic glasses based on convolutional neural network [J]. Journal of Non-Crystalline Solids, 2022, 595: 121846.

[35] CHAWLA N V, BOWYER K W, HALL L O, KEGELMEYER W P. Smote: Synthetic minority over-sampling technique [J]. Journal of Artificial Intelligence Research, 2002, 16: 321−357.

[36] ZHOU Z Q, HE Q F, LIU X D, WANG Q, LUAN J H, LIU C T, YANG Y. Rational design of chemically complex metallic glasses by hybrid modeling guided machine learning [J]. NPJ Computational Materials, 2021, 7(1): 138.

[37] BRANCO P, TORGO L, RIBEIRO R P. Exploring

resampling with neighborhood bias on imbalanced regression problems [C]//Proceedings in Artificial Intelligence, Heidelberg, Berlin: Springer, 2017: 513−524.

[38] BRANCO P, TORGO L, RIBEIRO R P. SMOGN: A pre-processing approach for imbalanced regression [C]//Proceedings of the First International Workshop on Learning with Imbalanced Domains: Theory and Applications. New York, NY: PMLR 74, 2017: 36−50.

[39] SUN Ya-juan, QU Dong-dong, HUANG Yong-jiang, LISS K D, WEI Xian-shun, XING Da-wei, SHEN Jun. Zr−Cu−Ni−Al bulk metallic glasses with superhigh glass-forming ability [J]. Acta Materialia, 2009, 57: 1290−1299.

领域知识指导的非晶合金非晶形成能力的机器学习

薄 宏[1]，陈旭东[1]，刘立斌[2]，方晓港[1]，胡建良[3]，王利民[1]

1. 燕山大学 亚稳材料全国重点实验室，秦皇岛 066004；
2. 中南大学 材料科学与工程学院，长沙 410083；
3. 燕山大学 机械工程学院，秦皇岛 066004

摘 要：为提高机器学习预测非晶形成能力的精度，从结构、热力学和动力学角度选取原子尺寸差、混合焓和估算的液相线温度处黏度作为特征参量。采用随机森林(RF)、极端梯度提升(XGBoost)和多层感知机(MLP)多种算法预测非晶合金的最大尺寸。结果表明，利用原始数据集和增强数据集建立的 XGBoost 模型都表现出了优异的性能，其中，后者在所有模型中取得了最高的决定系数 0.9148。由增强数据集训练的 XGBoost 模型预测的数据集之外的 Zr−Cu−Ni−Al−(Y)非晶合金的最大尺寸与测量值吻合最好，这表明其具有出色的泛化能力。通过模型解释发现，相比热力学和结构因素，动力学因素与非晶形成能力具有更强的相关性。

关键词：机器学习；极端梯度提升；Zr−Cu−Ni−Al−Y 合金；非晶形成能力；数据增强

(Edited by Xiang-qun LI)